applied sciences

MDPI

Article

Prediction of Corrosion Rate for Carbon Steel Using Regression Model with Commercial LPR Sensor Data

Kwang-Hu Jung [1] and Jung-Hyung Lee [2,*]

[1] Division of Cadet Training, Mokpo National Maritime University, Mokpo 58628, Republic of Korea; khjung@mmu.ac.kr
[2] Division of Marine System Engineering, Mokpo National Maritime University, Mokpo 58628, Republic of Korea
* Correspondence: jhlee@mmu.ac.kr; Tel.: +82-061-240-7205

Abstract: In this study, a model was proposed to predict the corrosion rate (Mils per Year, MPY) of carbon steel in a 3.5% NaCl solution, with the objective of comparing the effectiveness of a commercial LPR sensor against traditional electrochemical methods, using potentiostat-based LPR techniques. The primary factors considered in the experiments were temperature, flow velocity, and pH, tested through a full factorial design to identify the most influential variables. Statistical analysis showed that temperature and flow velocity had a significant effect on corrosion rate, with their interaction having the most substantial impact. In contrast, pH had no statistically significant influence within the tested conditions, likely due to the dominant effects of temperature and flow velocity in the high-salinity environment. The MPY data were validated through Tafel plots, immersion coupon tests, and other electrochemical techniques to confirm the reliability of the measurements. A regression model trained on 54 MPY data points demonstrated high accuracy, achieving a coefficient of determination (R^2) of 0.9733. The model also provided reliable predictions for factor combinations excluded from the training dataset. Additionally, scenario-based evaluations highlighted the model's performance under simulated operating conditions, while revealing challenges related to sensor contamination during long-term use. These findings emphasize the potential of commercial LPR sensors as effective tools for real-time corrosion monitoring and demonstrate the utility of the regression model in marine environments.

Keywords: carbon steel; corrosion rate; LPR sensor; electrochemical technique; regression model

check for updates

Citation: Jung, K.-H.; Lee, J.-H. Prediction of Corrosion Rate for Carbon Steel Using Regression Model with Commercial LPR Sensor Data. *Appl. Sci.* **2024**, *14*, 10836. https://doi.org/10.3390/app142310836

Academic Editor: Paolo Branchini

Received: 20 October 2024
Revised: 17 November 2024
Accepted: 21 November 2024
Published: 22 November 2024

Copyright: © 2024 by the authors. Licensee MDPI, Basel, Switzerland. This article is an open access article distributed under the terms and conditions of the Creative Commons Attribution (CC BY) license (https://creativecommons.org/licenses/by/4.0/).

1. Introduction

Carbon steel is a material widely employed in various industrial sectors due to its high strength and cost-effectiveness. It plays an essential role in structural components and piping systems, especially in the marine industry. Shipbuilding and offshore plants rely heavily on carbon steel for constructing hulls, pipelines, and infrastructure. However, the operating conditions in these environments are extremely harsh, and one of the most critical challenges in such applications is corrosion. Ships and power plants often utilize open-loop seawater cooling systems, where seawater acts as a cooling medium. In such systems, corrosion rate (CR) is influenced not only by the chemical composition of seawater but also by temperature and flow velocity, which vary with operating conditions.

Chloride ions in seawater accelerate electrochemical reactions that degrade metals [1,2], while variations in oxygen [3], pH [4], and salinity [5] add complexity. Higher temperatures in particular increase CRs by reducing activation energy [6], and faster flow velocities remove protective oxide layers. These factors accelerate CRs, compromising the service life of carbon steel, requiring effective corrosion management strategies. Thus, effective monitoring and management of corrosion are essential to prevent equipment degradation and ensure operational safety.

As the stability and service life of carbon steel degrade significantly under harsh conditions, corrosion management becomes important to minimizing operational risks and financial losses. Without proactive measures, corrosion can lead to unexpected equipment failures, downtime, and hazardous incidents. Globally, corrosion-related damages are estimated to cost $2.5 trillion annually—approximately 3.4% of the world's GDP (2013 data). Effective monitoring and early detection strategies could reduce these costs by 15–30%, emphasizing the importance of reliable corrosion management systems across various industries [7].

One of the key strategies for corrosion prevention is the introduction of early detection or monitoring systems, which can extend the service life of structures by identifying the corrosion risk in advance. Corrosion sensors are widely used for this purpose, especially in applications where access by personnel is limited, such as monitoring the inside of piping systems. These systems are increasingly complemented by automated data collection and remote monitoring technologies, allowing for continuous real-time analysis and early warning of potential corrosion risks. Such advancements are particularly beneficial in hazardous or hard-to-reach environments, where manual inspections are challenging, enhancing the overall efficiency of corrosion management.

The most common sensors are electrical resistance (ER) sensors and linear polarization resistance (LPR) sensors. ER sensors detect changes in electrical resistance due to the reduction in metal thickness and are useful for long-term corrosion loss measurement [8]. On the other hand, LPR sensors are suitable for real-time monitoring as they measure the small polarization resistance at the metal surface to determine instantaneous CRs [9].

Although corrosion detection sensors play an important role in preventing corrosion issues in various industries, their performance in harsh environments such as seawater systems is often limited. In such environments, multiple factors influence the durability and accuracy of these sensors. Open-loop seawater cooling systems used in ships and power plants pose additional challenges, as flow velocity and temperature fluctuations accelerate corrosion. Shin et al. [10] applied ER and LPR sensors as part of an algorithm study for measuring wall thickness reduction in carbon steel seawater pipes. Their studies revealed extremely high CRs in environments where flow velocity and temperature were key variables, with the sensors failing after approximately two weeks. Moreover, LPR sensors can report CRs up to 40% higher due to probe contamination in seawater [11]. This highlights the need for alternative approaches to corrosion monitoring that can overcome the challenges of sensors in dynamic and chemically aggressive seawater systems.

To overcome these challenges, various studies are exploring advanced approaches for improving sensor reliability. Machine learning-based algorithms and regression models have gained attention, as they incorporate environmental variables to predict CRs more accurately. Seghier et al. [12,13] applied ensemble learning and non-linear regression techniques to predict internal corrosion in oil and gas pipelines, while Peng et al. [14] proposed a machine learning algorithm for multiphase pipelines. Similarly, Dao et al. [15] developed a model using field data, achieving 93.22% accuracy in predicting damage from internal corrosion in gas pipelines.

Although machine learning techniques have shown promise in oil and gas pipelines, utilizing corrosion sensors for real-time monitoring in complex environments such as seawater remains limited. In seawater systems, multiple factors—chloride, oxygen, flow velocity, and temperature—interact, making accurate monitoring and prediction challenging. Corrosion sensors typically use electrodes made from the same material as the monitored target, such as carbon steel. However, in seawater, carbon steel can experience thickness losses of up to 1 mm per year [16], with higher flow velocities and temperatures accelerating the process. This not only impacts the monitored material but also degrades sensor electrode, reducing the electrode's lifespan and necessitating more frequent maintenance. As a result, measurement inaccuracies occur, undermining the effectiveness of real-time monitoring by corrosion sensor.

Developing predictive models or estimation equations based on key environmental variables, such as flow velocity, temperature, and pH, could provide a reliable method to assess corrosion rates without relying solely on sensors. These models would not only reduce the dependency on hardware prone to fouling and degradation but also offer a cost-effective and durable solution for long-term monitoring in harsh marine environments.

In this study, we aim to predict the CR of carbon steel in seawater pipes by developing a regression model for Mils per Year (MPY) based on flow velocity and temperature, using data obtained from a commercial LPR sensor. This approach will allow us to validate the reliability of LPR sensors in monitoring corrosion and evaluate the potential to predict long-term corrosion damage based on instantaneous CR.

2. Materials and Methods

2.1. Material and Specimen Preparation

The material used in the study was a mild steel, commonly employed in shipbuilding and piping system and structure. It was manufactured through a high-temperature hot rolling process followed by air-cooling. The chemical composition is detailed in Table 1. Specimens were machined to 20 × 9 × 6 mm (width, length, and thickness) dimensions to suitable both immersion and electrochemical testing. After machining, they were polished using grit SiC abrasive papers from #100 to #800, rinsed with distilled water, and oven-dried for storage to prevent contamination.

Table 1. Chemical composition (wt. %) of mild steel used for specimen preparation.

Chemical Composition (wt. %)										
C	**Si**	**Mn**	**P**	**S**	**Cu**	**Ni**	**Cr**	**Mo**	**Al**	**Fe**
0.19	0.13	0.62	0.02	0.007	0.01	0.01	0.01	0.01	0.031	Bal.

2.2. Full Factorial Design

The full factorial design was employed to investigate the complex interactions among three factors: temperature, flow velocity, and pH. The design involved three levels for each factor as shown in Table 2, and it was structured to simulate the conditions inside open circuit seawater cooling pipes. Each factor and their levels were set as follows:

(1) Temperature ranges [17]:

The temperature was set to reflect the surface seawater temperatures encountered during actual ship sailing, which generally range from 10 °C to 35 °C. However, within the seawater cooling system, the coolant temperature can rise up to 40 °C.

(2) Flow velocity ranges:

The flow velocity was set considering the actual conditions of seawater cooling pipes (max. 3.0 m/s) and the limitations of the experimental setup.

(3) pH ranges:

The pH of seawater typically ranges from 7.7 to 8.3, showing a slightly alkaline nature. However, due to increasing atmospheric CO_2 levels, ocean acidification is progressing, resulting in a downward trend in average seawater pH. Therefore, the pH range was set to 6–8.

Training, validation, and test data for the regression model were obtained using a full factorial design with three factors at three levels as shown in Table 2. The factor level was selected with consideration of the conditions inside seawater cooling pipes. This design incorporates experiments for all factor-level combinations as shown in Table 3, allowing identification of main effects and interactions. In Table 3, CR_{Com} and CR_{Pstat} represent the CR measured using the commercial sensor and potentiostat, respectively, and henceforth, CR values will be expressed as MPY for practical purposes.

Table 2. Experimental factors (temperature, flow velocity, and pH) and their levels used in the full factorial design.

Factors	Unit	Level			Response
Temperature	°C	10	25	40	
pH		6	7	8	CR (MPY)
Flow velocity	m/s	0.2	0.8	1.6	

Table 3. Experimental matrix showing all factor-level combinations for the full factorial design.

No.	Temperature	pH	Flow Velocity	$CR_{Com.}$, MPY	$CR_{Pstat.}$, MPY
1	10	6	0.2	37	37
2	10	6	0.8	56	52
3	10	6	1.6	65	62
4	10	7	0.2	35	28
5	10	7	0.8	48	47
6	10	7	1.6	66	60
7	10	8	0.2	37	42
8	10	8	0.8	47	53
9	10	8	1.6	67	61
10	25	6	0.2	57	50
11	25	6	0.8	99	87
12	25	6	1.6	122	117
13	25	7	0.2	47	42
14	25	7	0.8	78	80
15	25	7	1.6	123	124
16	25	8	0.2	63	57
17	25	8	0.8	81	76
18	25	8	1.6	138	141
19	40	6	0.2	67	72
20	40	6	0.8	127	127
21	40	6	1.6	187	179
22	40	7	0.2	78	76
23	40	7	0.8	112	111
24	40	7	1.6	174	163
25	40	8	0.2	84	79
26	40	8	0.8	130	123
27	40	8	1.6	187	172

A 3.5% NaCl solution was prepared using reagent-grade NaCl to replicate the typical seawater composition used in cooling systems. The temperature of the solution was controlled using a double-jacketed beaker connected to an external chiller, while the pH of the solution was adjusted with hydrochloric acid (HCl) and sodium hydroxide (NaOH) to achieve the desired pH levels. To simulate flow velocity, a 5 cm diameter of magnetic stir bar was rotated at three different speeds (80, 300, and 600 RPM) in a 1 L beaker containing 700 mL of NaCl solution using a high-speed stirrer. The flow velocity corresponding to each stirring speed was estimated using following equations:

$$\omega = RPM \times 2\pi/60 \quad (1)$$

$$v = \omega \times \gamma \quad (2)$$

where ω is the angular velocity, γ is the radial distance from the stir bar to beaker wall, and v is the linear velocity. The calculated flow velocities were approximately 0.2, 0.8, and 1.6 m/s. These values are approximations, as the calculation assumes simplified fluid dynamics, excluding factors such as beaker geometry, fluid viscosity, and turbulence.

2.3. CR Measurement

The CR was measured in MPY using a commercial two-electrode LPR sensor (CR-200 Wireless LPR corrosion Rate Sensor, Pyxis, COSASCO®, Santa Fe Spring, CA, USA) and a potentiostat (VSP potentiostat, Bio-Logic SAS, Grenoble, France). Figure 1 illustrate the experimental setup and specifications of the LPR sensor. This illustrates the setup of each test conducted in this study in single figure. The LPR sensor reading, immersion, and electrochemical tests were each conducted with independent experimental setups to prevent cross-influence between tests. The two-electrode LPR sensor used carbon steel electrodes (UNS K03005, COSASCO®, Santa Fe Spring, CA, USA), identical to the material used for the specimens in this study, and transmitted MPY readings via Bluetooth every 5 min. For each factor combination, the sensor reading was averaged once measurements stabilized, typically between 30 min and 1 h.

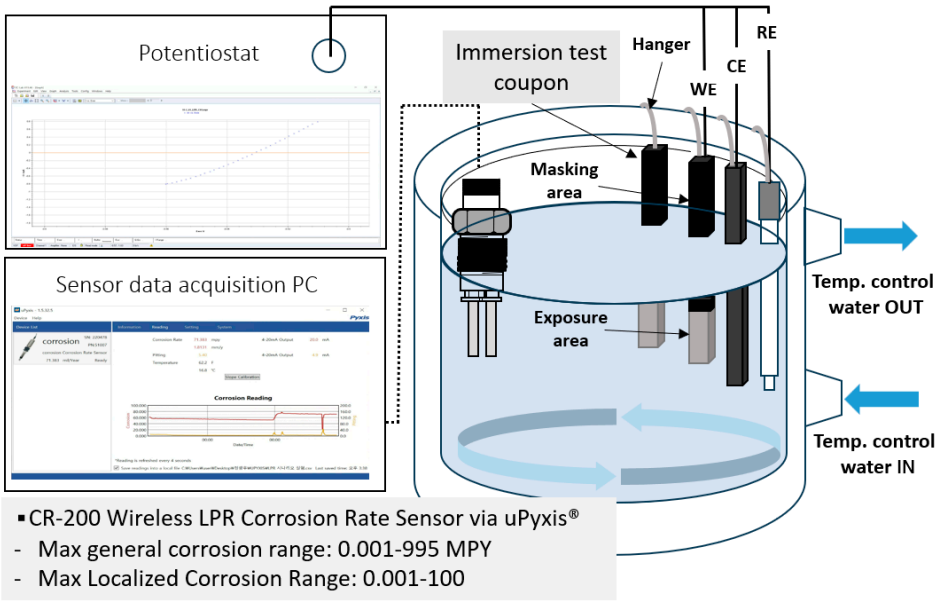


Figure 1. Experimental setup for CR measurement in MPY using commercial LPR sensor, potentiostat, and immersion test coupon.

To validate the sensor data, several electrochemical techniques were employed, including three-electrode LPR, potentiodynamic polarization, and various amplitude sinusoidal micro-polarization (VASP) techniques. These tests were conducted using a three-electrode corrosion cell consisting of a working electrode (specimen with an exposed area of 0.48 cm^2), a reference electrode (Ag/AgCl sat. KCl), and a counter electrode (graphite rod of Φ3.2). The cell was placed in a 1 L water jacketed beaker containing 700 mL of 3.5% NaCl solution.

The LPR test was performed to determine the polarization resistance (R_p). A small polarization was applied relative to the open-circuit potential (OCP), and the resulting current change was measured to calculate R_p, which is the ratio of the current response (Δi) to the polarization (ΔE), as shown in Equation (3) [18].

$$R_p = \Delta E / \Delta i \quad (3)$$

Using the Stern–Geary equation (Equation (4)) [18], the corrosion current density (I_{corr}) was derived:

$$I_{corr} = B / R_p \quad (4)$$

Here, B is the Stern–Geary constant, which is calculated from the Tafel slope using Equation (5) [18]:

$$B = (\beta_a \times \beta_c) / 2.3 \cdot (\beta_a + \beta_c) \quad (5)$$

where β_a and β_c represent the anodic and cathodic Tafel slope, respectively. The CR (MPY) was then calculated from $I_{corr.}$ using Faraday's law (Equation (6)) [18]:

$$CR\ (MPY) = (0.13 \times I_{corr.} \times EW)/\rho \quad (6)$$

In this equation, the 0.13 is a constant used to convert $I_{corr.}$ to CR (MPY). EW is the equivalent weight (27.93 g/equivalent for carbon steel), and ρ is the density (7.85 g/cm^3). All MPY values in this study were rounded to one decimal place for consistency. The LPR test was conducted by sweeping the potential from cathodic to anodic regions within a range of ±30 mV relative to the OCP, at a 0.5 mV/s scan rate. The $I_{corr.}$ was converted to specimen CR as MPY.

To complement the LPR data, the potentiodynamic polarization test was conducted by sweeping the potential across a broader range, specifically within ±300 mV of the OCP at the same scan rate. This technique allowed for a more detailed analysis of corrosion behavior by extrapolating the anodic and cathodic Tafel slopes to determine I_{corr}.

Lastly, the VASP technique [19] was employed to validate the corrosion data non-destructively. Like LPR, VASP provides non-destructive and instantaneous measurements, making it highly effective for real-time corrosion monitoring. However, VASP is a relatively new technique and has not yet been fully validated across a wide range of applications, which introduces uncertainties regarding its reliability. This technique, based on electrochemical impedance spectroscopy (EIS), uses low-voltage amplitude perturbation to determine both the CR and Tafel parameters without damaging the sample surface. In this study, the VASP test was conducted at a 0.23 Hz frequency and 20 sinus amplitude.

2.4. Immersion Test for the Corrosion Coupons

To further validate the CR obtained through the LPR technique, an immersion corrosion test was performed on corrosion coupons. This test allowed for the comparison of electrochemical measurements with actual corrosion damage depth, providing additional validation of the LPR-based MPY readings. The corrosion damage depth was measured using a 3D laser confocal microscope (OLS 5000, OLYMPUS, Tokyo, Japan), which determined the step height between the masked and exposed areas on the coupon surface. The measured depth values (μm) were subsequently converted to MPY for direct comparison with the electrochemical results.

2.5. Statistical Analysis

The experimental data were analyzed using Minitab 19 statistical software. In the regression modeling process, the MPY values obtained from the full factorial design served as the response variable. To ensure the reliability of the model, 5-fold cross-validation was employed during the training phase, and the model was refined using stepwise regression to identify significant factors. The analysis of variance (ANOVA) was conducted to determine the significance of factors at a 95% confidence level, ensuring the robustness of the results.

2.6. Experimental Assumptions

In this study, the experimental conditions were controlled for temperature, flow velocity, and pH to investigate their effects on the CR of carbon steel. However, in comparison to these controlled variables, pH range, salinity, and dissolved oxygen (DO) were treated as fixed or assumed based on typical seawater environments. The following assumptions were made:

(1) pH ranges:

While the pH was controlled within the range of 6 to 8, this range reflects natural seawater conditions, where significant deviations are uncommon. Outside this range, corrosion behavior can change, but within it, carbon steel exhibits a relatively stable CR, minimizing the effect of pH on CR.

(2) Fixed salinity:

The salinity was set at 3.5 wt. % NaCl, representing the typical seawater concentration. CR generally increases with salinity until reaching a critical threshold near 5 wt. %, beyond which further increases in salinity tend to reduce CR. Thus, variations beyond 3.5 wt. % are assumed to have no significant effect on corrosion behavior under the tested conditions.

(3) Dissolved oxygen:

Dissolved oxygen was not explicitly controlled during the experiments, as open-circuit seawater cooling systems naturally replenish oxygen through continuous contact with the atmosphere. Therefore, oxygen availability was assumed to remain sufficient, ensuring that the corrosion process was not limited by oxygen depletion.

The above assumptions simplify the experimental setup, enabling a focused investigation into how temperature, flow velocity, and pH influence the CR of carbon steel.

3. Results and Discussion

3.1. Summary of Experiment Results

The experimental results, presented in Figure 2, summarize the CR (MPY) values obtained across various factor combinations listed in Table 3, measured using both a commercial LPR sensor and a potentiostat. The data showed a clear correlation between temperature, flow velocity, and CR: higher temperatures and faster flow velocities resulted in increased MPY values. The most severe MPY values were recorded under the highest levels of temperature and flow velocity (No. 21, 24, and 27).

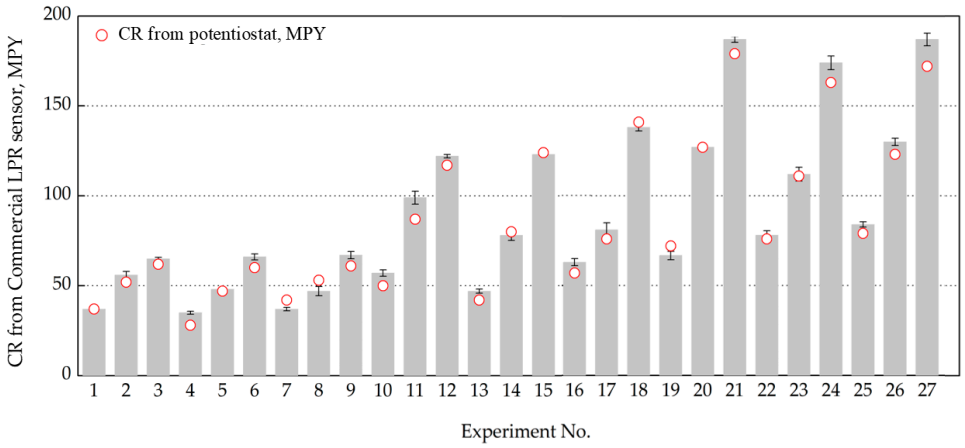


Figure 2. CR values obtained from LPR tests for the factor combinations shown in Table 3.

In contrast, pH levels between 6 and 8 did not exhibit a significant impact on MPY under the tested conditions. This suggests that the CR of carbon steel remains stable within the tested pH range, confirming that temperature and flow velocity are dominant factors influencing corrosion under seawater conditions. The results also demonstrate the agreement between the commercial LPR sensor and the potentiostat measurements, with both techniques yielding MPY values within the standard deviation. This consistency demonstrates that the use of two-electrode LPR sensors as a reliable alternative to three-electrode systems for real-time corrosion monitoring.

3.2. Statistical Analysis of Factor Effects on CR

Figure 3 presents a Pareto chart that graphically confirms the statistical significance of each factor—temperature (A), flow velocity (C), and their interaction (A·C) on the CR. The chart uses standardized effects to show the influence of these factors, with the red dashed line representing the Bonferroni-corrected threshold. Any factor or interaction exceeding this line is considered statistically significant within the 95% confidence interval ($\alpha = 0.05$) and must be included in the regression model. The chart illustrates that temperature (A),

flow velocity (C), and their interaction (A·C) are the most significant factors influencing CR. Other factors such as pH or interactions did not exceed the significance threshold and are therefore not considered important in this study. This indicates that the CR of carbon steel is primarily driven by the interaction between temperature and flow velocity, rather than by the independent effect of each factor alone.

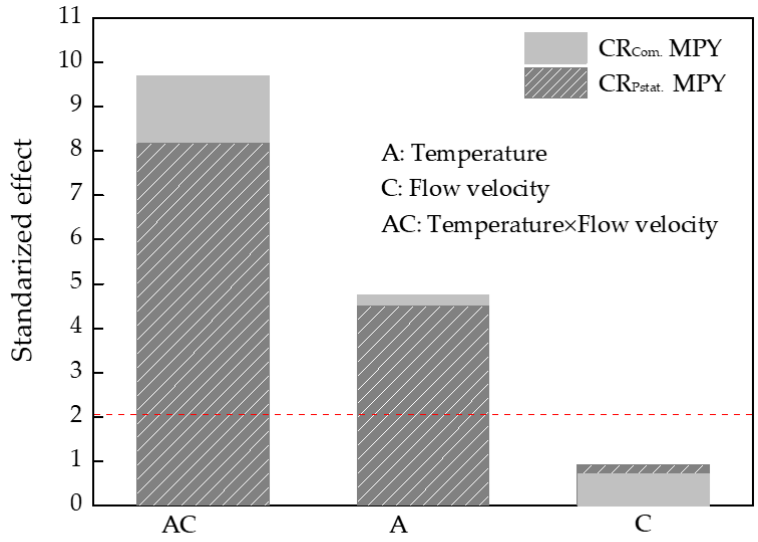


Figure 3. Pareto chart of the standardized effects for significant factors in 95% confidence level.

ANOVA is a statistical method used to compare two or more groups by examining the variance within and between groups, determined by the total mean and the differences in mean between groups. It facilitates the assessment of each independent variable's significant influence on the corrosion rate, which is essential for validating the effectiveness of the regression model. In ANOVA, the mean of square (MS) is calculated by dividing the sum of squares (SS) by the degrees of freedom (DF). The F-value is defined as the ratio of the MS to the error mean square, and it reflects the influence of a factor within the model. A high F-value indicates a stronger influence on the response variable. The *p*-value is the most important characteristic in ANOVA, as it determines whether a factor has a significant effect. At a 95% confidence level ($\alpha = 0.05$), a *p*-value less than 0.05 indicates that the factor is statistically significant.

The ANOVA results (Table 4) showed that the overall regression model is highly significant, with an F-value of 373.81 and $p < 0.001$, indicating that the included factors explain a substantial portion of the variability in CR. Among the individual factors, temperature was found to have a significant effect on CR ($F = 24.58$, $p < 0.001$), while flow velocity alone was not significant ($F = 0.54$, $p = 0.47$). However, the interaction between temperature and flow velocity was highly significant ($F = 94.89$, $p < 0.001$), confirming that the effect of temperature on CR is heavily dependent on the flow velocity.

Table 4. Results of ANOVA for significant terms in regression model.

	DF	Adj. SS	Adj. MS	F-Value	*p*-Value
Regression	3	52,479.7	17,493.2	373.81	0.000
Temp.	1	1150.3	1150.3	24.58	0.000
Velocity	1	25.3	25.3	0.54	0.47
Temp × Velocity	1	4440.4	4440.4	94.89	0.000
Error	23	1076.3	46.8		
Sum	26	53,556.0			

Figure 4 illustrates the interaction effect between temperature and flow velocity, demonstrating that both factors accelerate the CR when combined. At a flow velocity of 1.6 m/s, the rapid removal of corrosion products from the metal surface enhanced the oxygen supply, which further accelerated corrosion [20]. This effect became particularly pronounced when the temperature reached 40 °C, accelerating the CR due to the synergistic interaction between high temperature and fast flow velocity.

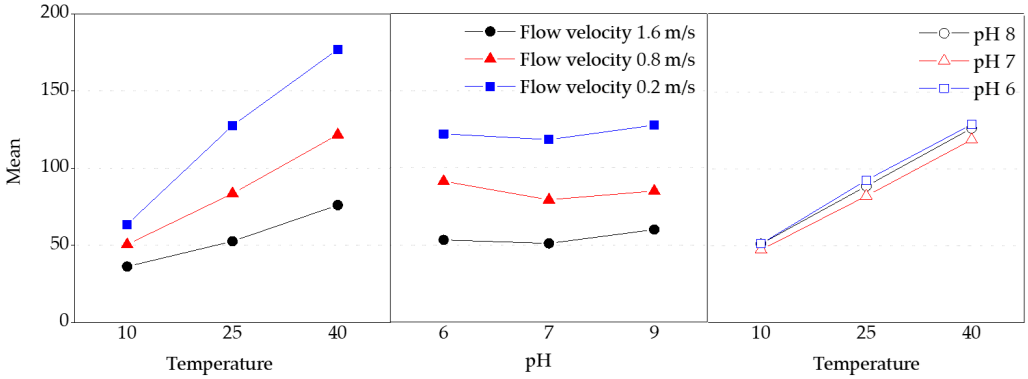


Figure 4. Interaction effects of temperature, flow velocity, and pH on MPY.

On the other hand, pH did not result in a significant difference in CR as a level change. This suggests that carbon steel exhibits relatively stable corrosion characteristics in seawater at pH levels within the range of 6 to 8. According to fundamental principles of corrosion chemistry, the CR of carbon steel typically decreases as pH increases [21,22]. Previous research has identified pH as an influencing factor for CR. Chohan et al. [23] reported that lowering the pH level of seawater from 8.5 to 7.0 increased the CR by 42.52%. Similarly, Wang et al. [24] found that CR accelerates in acidic environments, indicating that lower pH levels lead to more aggressive corrosion behavior. However, the results of this study indicate that in the presence of temperature and flow velocity factors in a 3.5% NaCl solution, the influence of pH is not significant.

3.3. Validation of MPY Data Through Electrochemical Techniques

The reliability of the MPY data, which is critical for the accuracy of the regression model, was validated through multiple electrochemical techniques: Tafel extrapolation, VASP, and LPR tests. These methods provide complementary insights into corrosion behavior, ensuring the robustness of the data.

The Tafel extrapolation method, a traditional technique, was used to estimate the corrosion current density (I_{corr}) and calculate the CR. Figure 5 presents the potentiodynamic curves plotted at flow velocities of 0.2 m/s, 0.8 m/s, and 1.6 m/s at 25 °C. As the flow velocity increased, the curves shifted the corrosion potential in the anodic direction, indicating enhanced oxygen diffusion to the metal surface and reduced concentration polarization [25,26]. This behavior corresponds with the increased removal of iron oxide from the metal surface, leading to a higher CR. Specifically, at static conditions, the corrosion potential of carbon steel was −0.65 V, consistent with the potential of iron oxide formation on the surface [27]. As the flow velocity increased from 0.2 m/s to 1.6 m/s, the corrosion potential shifted from −0.54 V to −0.48 V, and I_{corr} also exhibited an upward trend, corresponding with the results from the LPR tests.

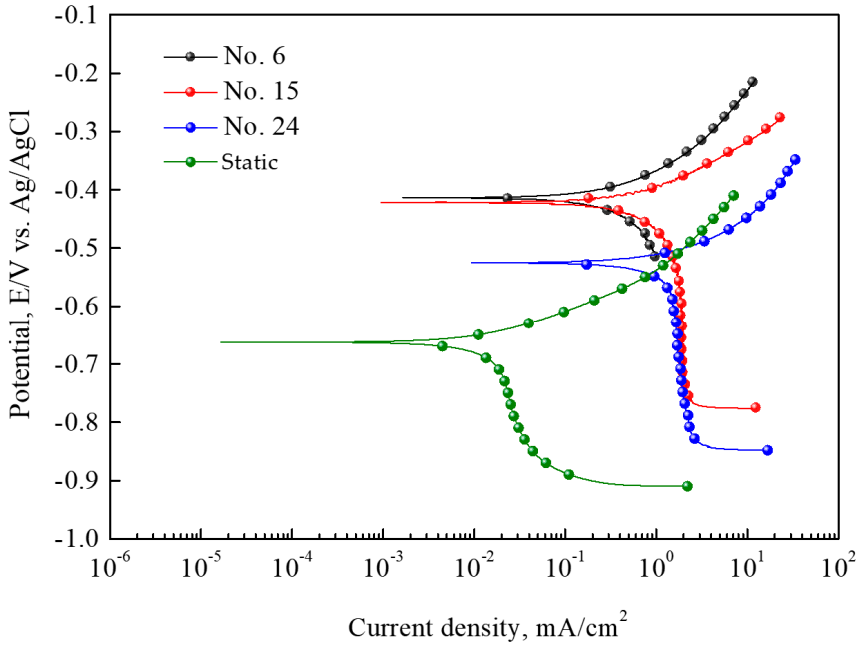


Figure 5. Potentiodynamic polarization curves at various flow velocities (static, 0.2 m/s, 0.8 m/s, and 1.6 m/s) measured at 25 °C.

In addition to Tafel extrapolation, the VASP technique was employed to further validate the MPY data. Figure 6 compares the CR measured by LPR, Tafel extrapolation, and the VASP technique under nine different factor combinations, where only temperature and flow velocity were varied. These experiments were conducted using a neutral 3.5% NaCl solution, with the pH factor intentionally excluded to isolate the effects of temperature and flow velocity on CR.

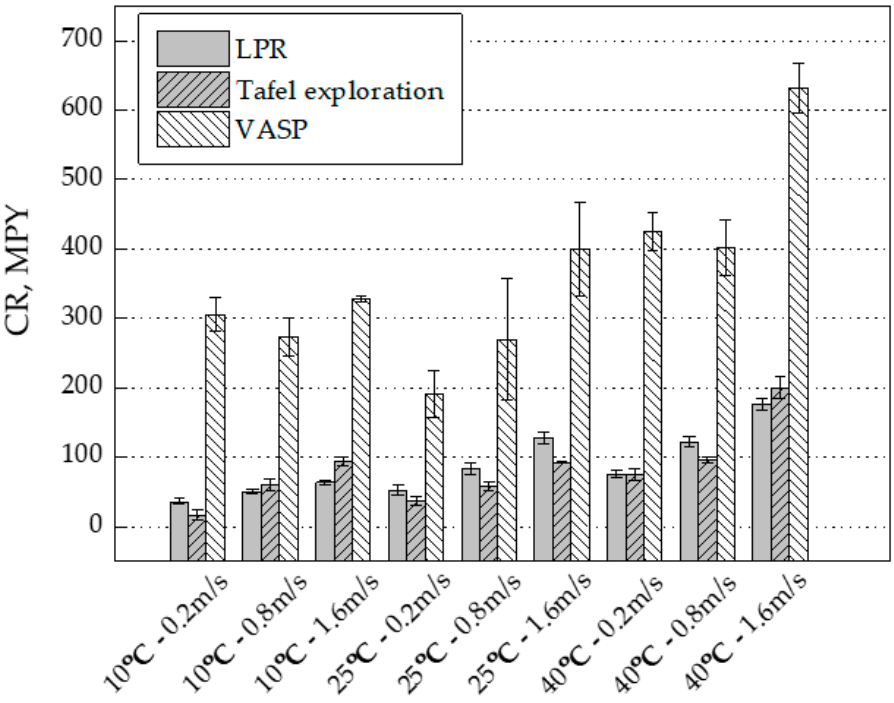


Figure 6. Comparison of CR measured by LPR, Tafel extrapolation, and VASP techniques under nine factor combinations, where only temperature and flow velocity varied.

Both LPR and Tafel extrapolation techniques demonstrated that the CR increased with temperature and flow velocity, with both methods producing similar results. However, slight differences were observed due to the fundamental differences between the techniques. LPR measures corrosion current within a small polarization range, while Tafel extrapolation estimates corrosion current over a broader polarization range [28]. As a result, Tafel extrapolation often provides a more precise estimation of corrosion current, but it can introduce errors due to the experimenter's judgment during curve fitting and calculation.

The VASP technique, however, yielded MPY values at least three times higher than the other electrochemical techniques. This disparity is attributed to the non-linear responses detected by VASP across a wider polarization range. While VASP is effective for evaluating corrosion resistance in coatings through electrochemical impedance spectroscopy (EIS), it is less suitable for bulk metal corrosion measurements [29,30]. These results indicate that VASP may measure additional phenomena not directly related to the corrosion of carbon steel in this context, rendering it unsuitable for the present study.

3.4. Validation of MPY Data Through Immersion Testing of Corrosion Coupons

The immersion test was conducted to verify the MPY values obtained from the LPR sensor by comparing them with the actual material loss measured on corrosion coupons. The coupons were immersed in a neutral 3.5% NaCl solution at 25 °C for up to 60 h. After the immersion period, the corroded surface profiles were analyzed using a 3D laser confocal microscope. The microscope provided detailed surface topography, measuring the difference in elevation between the masked area (non-corroded) and the corroded area, indicating the extent of metal loss due to uniform corrosion. This vertical depth difference was then converted into MPY values for comparison with the LPR sensor readings. The measured depth was converted to MPY values according to the relationship to Equation (7).

$$MPY = um/year \times 0.03937 \quad (7)$$

In Figure 7, the colors represent the difference in elevation between the masked area (non-corroded) and the corroded area. As shown in Figure 7, the corrosion profiles illustrate the smooth transition between the masked and corroded areas, confirming that the corrosion observed corresponds to general corrosion (uniform corrosion) rather than localized corrosion such as pitting and crevice corrosion. The measured depth ranged between 23 μm and 47 μm, though these specific values are not significant for analysis. Instead, the masked area serves as a stable reference point to accurately measure the vertical material loss in the corroded regions, which is more relevant for evaluating uniform corrosion behavior. The MPY values derived from these measurements were then compared with the LPR sensor readings. For example, profile (a) shows an actual CR of 119 MPY, while the LPR sensor reported 127 ± 10 MPY, demonstrating good agreement. Similarly, in profiles (c) and (d), the actual CR values were 186 and 174 MPY, respectively, with corresponding LPR readings of 171 ± 17 MPY and 171 ± 7 MPY, reflecting the reliability of the sensor across multiple conditions. These results confirm that the LPR sensor provides reliable estimates of CR, even in short-term tests, with minor discrepancies attributed to surface roughness and measurement variability.

The immersion test validates the practicality of LPR sensors for real-time corrosion monitoring, as the instantaneous MPY values closely match the material loss recorded during immersion. The consistent performance of the sensor demonstrates its capability to detect general corrosion trends effectively, making it suitable for use in environments such as marine cooling systems where continuous corrosion monitoring is essential.

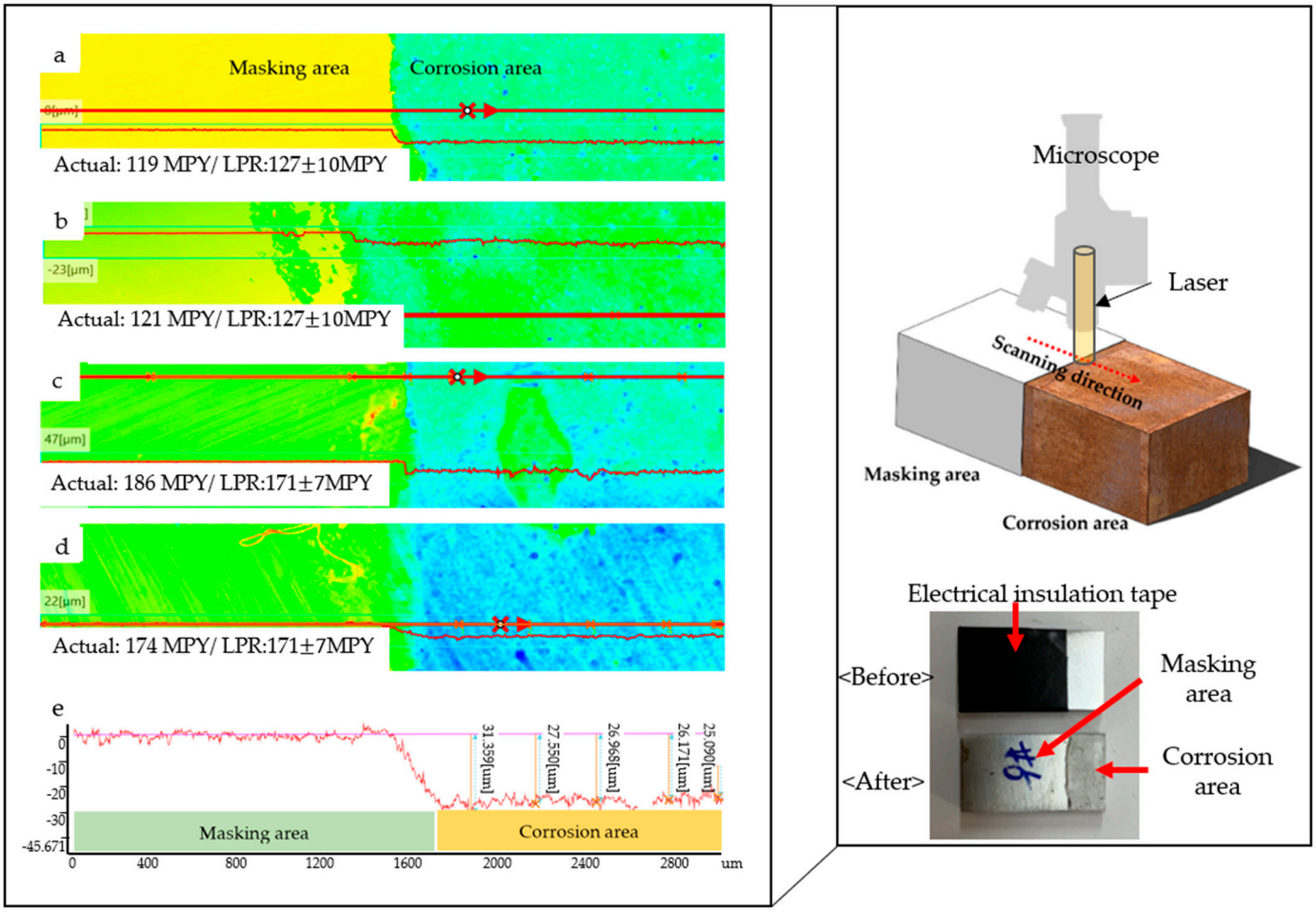


Figure 7. Three-dimensional surface profiles of corrosion coupons tested in a 3.5% NaCl solution with pH fixed at 7 and flow velocity at 1.6 m/s: (**a**) 25 °C for 48 h, (**b**) 25 °C for 60 h, (**c**) 40 °C for 48 h, (**d**) 40 °C for 60 h. (**e**) Surface analysis of profile for (**d**).

3.5. Development and Training of the Regression Model

Figure 8 presents the experimental results, showing the relationship between the factors (temperature and flow velocity) and the response variable (CR, MPY). This study aimed to determine whether these relationships are linear or non-linear and to establish the relative importance of each factor in the regression model. The results indicate that CR increases non-linearly with flow velocity, exhibiting behavior close to second-order trends. Additionally, the effect of temperature on the CR follows an exponential trend, consistent with the Arrhenius equation [31]. These findings demonstrates the necessity of incorporating interaction terms in the regression model to account for the combined influence of temperature and flow velocity on corrosion behavior.

The regression models developed using the data from the commercial LPR sensor and the potentiostat are expressed as follows:

$$MPY_{com.} = 22.3 + 0.9666temp + 3.84vel + 1.826temp * vel \left(R^2 = 0.9764\right) \quad (8)$$

$$MPY_{pstat.} = 20.17 + 0.992temp + 5.28vel + 1.676temp * vel \left(R^2 = 0.9672\right) \quad (9)$$

These equations reflect the contributions of temperature, flow velocity, and their interaction (temp·vel) to the MPY values. Here, temp is expressed in degrees Celsius, and vel in meters per second. The interaction term addresses the non-linear relationship between the two factors, showing how their combined effect differs from their individual

contributions. This approach helps better represent the complex corrosion dynamics in environments such as marine cooling systems.

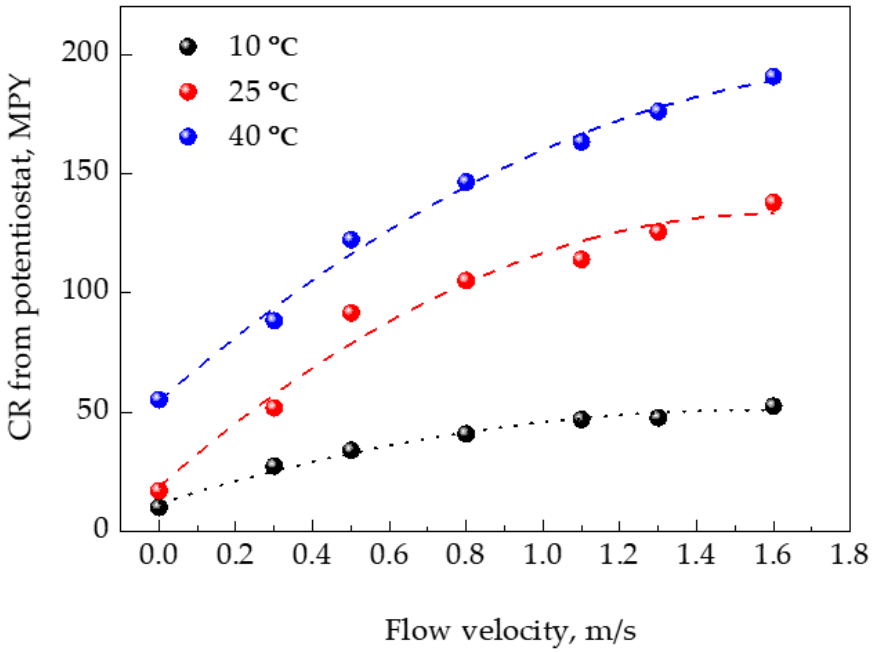


Figure 8. CR measured by potentiostat as a function of flow velocity and temperature.

The coefficient of determination (R^2) for each model, calculated using Equation (10), evaluates the model's performance:

$$R^2 = 1 - \frac{\sum (y_i - \hat{y}_i)^2}{\sum (y_i - \overline{y})^2} \tag{10}$$

where y_i represents the actual MPY values, $\hat{y}_i$ is the predicted values from the model, and $\overline{y}$ is the mean of the responses. An R^2 value close to one indicates that the models explain most of the variability in the data, confirming their reliability.

Both models demonstrate high R^2 values (0.9764 for the LPR sensor and 0.9672 for the potentiostat), indicating a strong fit with the training data. Moreover, the constants and weights in both models are nearly identical, further validating the consistency of the data obtained from the two measurement methods. This consistency supports the use of LPR sensors as practical alternatives to the three-electrode corrosion cells, offering comparable accuracy in monitoring CR in real-time.

To enhance the model's robustness and reduce overfitting, the datasets from both techniques were combined into an integrated regression model with 54 samples:

$$MPY_{model} = 21.26 + 0.977temp + 4.54vel + 1.725temp * vel \ (R^2 = 0.9733) \tag{11}$$

The integrated model provides a balanced prediction of CR by drawing on data from both measurement techniques. The interaction term in the model remains significant, emphasizing the importance of simultaneously accounting for both temperature and flow velocity when predicting corrosion behavior. With an R^2 of 0.9733, the integrated model explains almost all variability in the data, demonstrating its reliability for practical applications.

The stepwise regression process ensured that only statistically significant terms were retained, resulting in a more interpretable model. Higher-order terms were excluded, as they did not meaningfully contribute to the predictions. The final models confirm that

temperature, flow velocity, and their interaction are the primary factors influencing CR, consistent with the observations in Figure 8.

The results show that LPR sensors are reliable tools for real-time corrosion monitoring, providing MPY data comparable to traditional potentiostat measurements. The integrated model offers a practical solution for applications that demand continuous monitoring, such as marine seawater cooling systems. In these environments, understanding the relationship between temperature and flow velocity plays an imperative role in preventing equipment degradation and maintaining operational performance.

3.6. Validation of the Regression Model

The predictive performance of the regression model was evaluated by comparing its predictions with experimental data that were excluded from the training dataset. This assessment was essential to confirm the model's ability to generalize to new data while avoiding overfitting, despite its high fit with the training data (R^2 = 0.9733).

Table 5 presents a comparison between the predicted MPY values from the model and the actual MPY values measured by the commercial LPR sensor and potentiostat. Each predicted value is accompanied by a prediction interval (PI), representing the range within which the actual values are expected to fall with a high degree of confidence.

Table 5. Comparison of predicted CR with experimental results from commercial LPR sensor and potentiostat for validation.

	Temp	Flow Velocity	CR_{model} (PI), MPY	CR_{com}, MPY	CR_{Pstat}, MPY
Test 1	15	0.4	48 (33~63)	38	45
Test 2	30	1.2	119 (104~133)	127	131
Test 3	20	1.6	104 (89~119)	113	102
Test 4	35	0.27	73 (58~88)	65	75

The data in Table 5 demonstrate that the predicted MPY values remain within the expected range for all test conditions, as indicated by the prediction intervals (PIs). This consistency shows that the model is capable of making reliable predictions, even when applied to new factor combinations not included in the training dataset. For example, in Test 2, the model predicted 119 MPY (PI: 104–133), while the actual values were 127 MPY from the sensor and 131 MPY from the potentiostat—both comfortably within the predicted range. Although minor discrepancies were observed, such as in Test 1 where the model predicted 48 MPY (PI: 33–63) but the actual readings were slightly lower (38 MPY from the sensor and 45 MPY from the potentiostat), these variations fall within an acceptable margin. This suggests that the model maintains predictive consistency across various operating conditions.

At lower flow velocities and higher temperatures, as seen in Test 4, the model tends to slightly overestimate MPY values. This behavior indicates that incorporating additional data points at intermediate levels may further enhance the model's accuracy by refining its ability to represent non-linear trends effectively. Overall, the agreement between predicted and observed MPY values validates the robustness of the model. The results confirm that the predictions are reliable and remain within the expected range for new conditions, making the model a practical tool for real-time corrosion monitoring.

3.7. Evaluation Under Simulated Operating Conditions

The model undergoes practical validation through tests simulating real-world conditions in cooling seawater pipes within a ship engine room. These simulations account for dynamic factors such as engine load, regional sea surface temperature, and energy-saving operations, reflecting the complex environment in which corrosion monitoring is required. The test protocol followed the same procedure described in Section 2.3.

The simulation consisted of 15 sequential steps, with temperature and flow velocity adjusted according to the factor levels used in this study. Figure 9 illustrates the progression

of CR predictions over time as these operating conditions change. Test coupons were used to measure actual metal loss at five major points throughout the simulation, providing a benchmark for validating the model's accuracy. The detailed results for each stage are presented in Table 6.

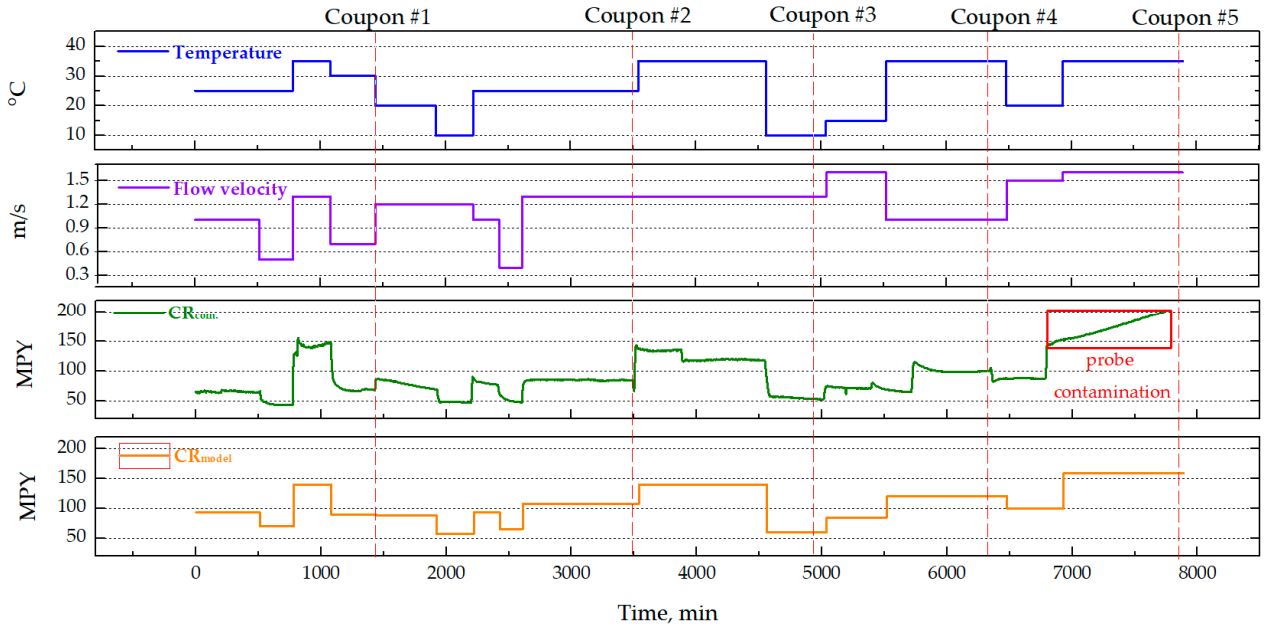


Figure 9. CR predictions and measurements across sequential operating conditions with varying temperature and flow velocity.

Table 6. Scenario-based comparison of CR predictions from the regression model and measurements from the commercial LPR sensor. Factor combinations used in the scenario were excluded from the training data.

Step	Factor		CR_{comm}, MPY	CR_{model}, MPY
	Temperature, °C	Flow Velocity, m/s		
1	25	1	65 ± 1	93
2	25	0.5	46 ± 7	70
3	35	1.3	141 ± 5	140
4	30	0.7	70 ± 8	90
5	20	1.2	78 ± 5	88
6	10	1.2	50 ± 7	57
7	25	1	79 ± 4	93
8	25	0.4	56 ± 7	65
9	25	1.3	84 ± 8	108
10	35	1.3	124 ± 8	140
11	10	1.3	57 ± 11	59
12	15	1.6	71 ± 5	85
13	35	1	89 ± 16	120
14	20	1.5	87 ± 3	99
15	35	1.6	170 ± 17	159

The data in Table 6 confirm that the model's predictions closely correspond to the measured CR from the test coupons. For instance, at Step 10, the predicted CR was 112 MPY, while the actual measurement was 110, indicating strong agreement. However, at lower flow velocities, such as in Step 12, the model showed a slight overestimation (89 predicted vs. 85 measured). This pattern suggests that the model may benefit from additional data at intermediate factor levels to identify non-linear trends more accurately.

In Step 15, the CR increased steadily over time, but this rise was not due to corrosion acceleration. Instead, it resulted from probe contamination caused by prolonged exposure to the harsh environment. This observation emphasizes the necessity of considering sensor fouling in long-term corrosion monitoring, as contamination can lead to gradual shifts in MPY readings and affect accuracy [10,11].

Figure 10 shows the cumulative general corrosion depth over the simulation period, derived from the CR predictions. The results demonstrate that the model effectively tracks the trends in CR under varying conditions. Although minor overestimation was observed toward the later steps, the predicted CR maintained good consistency with both the coupon measurements and the readings from the commercial LPR sensor at the final stage (Coupon #5).

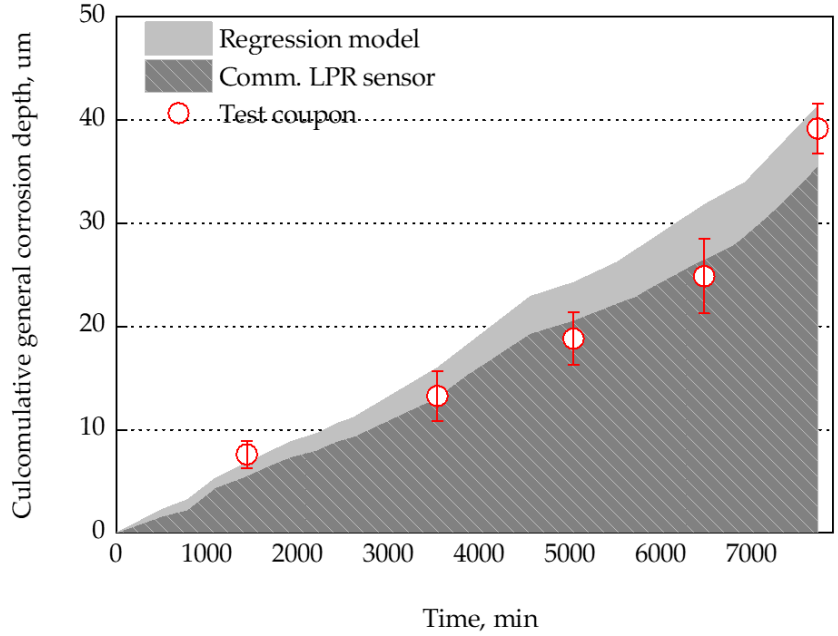


Figure 10. Cumulative corrosion depth over time: comparison between predictions from the regression model, readings from the commercial LPR sensor, and measurements from test coupons.

The ability to provide reliable predictions across multiple scenarios emphasizes the practical value of the regression model. By integrating the effects of temperature and flow velocity, the model offers a powerful tool for continuous corrosion monitoring in dynamic environments. The study shows that accurate prediction of CRs can help operators anticipate equipment degradation and implement preventive actions proactively, reducing the risk of unexpected failures.

4. Conclusions

This study evaluated the effects of the interaction between temperature, flow velocity, and pH on the CR (MPY) of carbon steel in a 3.5% NaCl solution. The experimental results indicated that both temperature and flow velocity had a significant effect on the CR, while the interaction between these two factors had the greatest effect. Our findings extend beyond previous research by quantitatively demonstrating that this interaction contributes the most to the MPY variance, whereas previous research typically focused on individual factor influences.

On the other hand, pH did not have significant effect on the MPY, which is a somewhat different result compared to previous studies. While earlier research has reported significant pH influences on corrosion rates, our findings indicate that under high-salinity conditions with variable temperature and flow, the effect of pH is statistically negligible.

This suggests that corrosion management strategies in seawater cooling systems should prioritize temperature and flow control over pH adjustment.

The comparison between the two-electrode commercial LPR sensor and the three-electrode potentiostat system revealed consistent MPY values across various factor combinations tested under the full factorial design. By incorporating multiple validation techniques, our approach offers a more robust framework than traditional single-method approaches. The MPY data were further validated through Tafel plots and immersion coupon tests, confirming the reliability of both measurement methods. The regression model, trained with 54 datasets, achieved an R^2 of 0.9733, indicating a high level of accuracy in explaining the variability in MPY. This represents a significant improvement over previous predictive models, especially in terms of real-time monitoring applications.

Despite the promising results, this study has several limitations:

1. The dataset was constrained to the factor levels and conditions tested, which may limit the model's ability to capture more complex, non-linear patterns beyond the tested ranges.
2. While short-term validation was performed, long-term monitoring in real-world marine systems remains necessary to ensure the robustness of the model over time.
3. pH variations in different environments may require further investigation to better understand their potential effects under varying salinity levels.
4. The effects of sensor contamination during extended use need more detailed investigation.

The simulated operating condition tests further validated the model's predictive performance. These tests highlighted the potential of the LPR sensor for real-time corrosion monitoring but also revealed challenges, such as probe contamination during long-term use in marine environments. This observation highlights the importance of regular maintenance protocols and enhanced sensor designs for long-term use.

In conclusion, this study provides valuable insights regarding the interaction between temperature, flow velocity, and pH in predicting and monitoring the corrosion rate of carbon steel in marine environments. The integrated model developed here contributes to the advancement of corrosion monitoring systems, offering a tool for improving maintenance strategies and reducing the risks of equipment degradation. By connecting laboratory findings with practical applications, our research provides a broader framework for understanding and managing corrosion in marine environments. With further research and long-term validation, the methods proposed in this study have the potential to play an important role in improving the reliability and efficiency of corrosion management in marine applications.

5. Future Work

Future studies should focus on conducting long-term validation using a lab-scale piping system to better simulate real-world operating conditions over extended periods. This setup would allow for continuous monitoring of corrosion behavior while assessing the model's ability to predict CRs under more dynamic conditions, such as fluctuating temperature and flow velocity. Furthermore, expanding the dataset with more diverse factor levels and environmental conditions would enhance the model's ability to detect non-linear trends. Research into sensor fouling mitigation strategies and automated cleaning mechanisms will also be critical to improving the long-term performance of LPR sensors in harsh marine environments.

A crucial area for future investigation is the comprehensive study of sensor fouling mechanisms and their long-term effects on measurement accuracy. While this study identified sensor contamination as a significant challenge, deeper research is needed to understand both corrosion-induced fouling (such as oxide film formation and degradation of electrode surfaces) and marine fouling (including biological growth and mineral deposits). These fouling mechanisms may interact differently under various environmental conditions, such as seasonal temperature fluctuations and varying salinity levels, potentially

affecting sensor readings in complex ways. Future research should focus on developing robust solutions that address both types of fouling, possibly through improved electrode materials, smart cleaning systems, and advanced signal processing algorithms for compensating measurement drift. Such developments would significantly improve the reliability of long-term corrosion monitoring in marine environments using LPR.

Author Contributions: Conceptualization, K.-H.J. and J.-H.L.; methodology, K.-H.J.; software, K.-H.J.; validation, K.-H.J. and J.-H.L.; formal analysis, K.-H.J.; investigation, K.-H.J. and J.-H.L.; resources, K.-H.J. and J.-H.L.; data curation, K.-H.J.; writing—original draft preparation, K.-H.J.; writing—review and editing, K.-H.J. and J.-H.L.; visualization, K.-H.J.; supervision, J.-H.L.; project administration, J.-H.L.; funding acquisition, J.-H.L. All authors have read and agreed to the published version of the manuscript.

Funding: This work was supported by the "Autonomous Ship Technology Development Program (20011164, Development of Performance Monitoring and Failure Prediction and Diagnosis Technology for Engine System of Autonomous Ships)" funded by the Ministry of Trade, Industry & Energy (MOTIE, Korea).

Institutional Review Board Statement: Not applicable.

Informed Consent Statement: Not applicable.

Data Availability Statement: The data presented in this study are available on request from the corresponding author. The data are not publicly available due to the project requirements.

Conflicts of Interest: The authors declare no conflicts of interest.

References

1. Costa, R.D.; Barbosa, M.L.; Silva, F.J.; Sousa, S.R.; Sousa, V.F.; Ferreira, B.O. Study of the chlorine influence on the corrosion of three steels to be used in water treatment municipal facilities. *Materials* **2023**, *16*, 2514. [CrossRef] [PubMed]
2. Brownlie, F.; Hodgkiess, T.; Pearson, A.; Galloway, A. Electrochemical evaluation of the effect of different NaCl concentrations on low alloy-and stainless steels under corrosion and erosion-corrosion conditions. *Corros. Mater. Degrad.* **2022**, *3*, 101–126. [CrossRef]
3. Eyu, G.D.; Will, G.; Dekkers, W.; MacLeod, J. Effect of dissolved oxygen and immersion time on the corrosion behaviour of mild steel in bicarbonate/chloride solution. *Materials* **2016**, *9*, 748. [CrossRef]
4. Sarmiento, A.M.; Rodriguez-Perez, A.M.; Davila, J.M.; de la Torre, M.L. Effect of acid mine drainage on the mechanical properties of AISI 1020 carbon steel and AW6060 aluminium. *J. Mater. Res. Technol.* **2024**, *32*, 541–549. [CrossRef]
5. Smith, F.; Brownlie, F.; Hodgkiess, T.; Toumpis, A.; Pearson, A.; Galloway, A.M. Effect of salinity on the corrosive wear behaviour of engineering steels in aqueous solutions. *Wear* **2020**, *462*, 203515. [CrossRef]
6. Wang, L.; Gao, Z.; Liu, Y.; Lu, X.; Wang, C.; Hu, W. Effect of temperature on corrosion behavior of X65 steel in simulated deep sea environment. *Int. J. Electrochem. Sci* **2019**, *14*, 161–172. [CrossRef]
7. Koch, G. Cost of corrosion. In *Trends in Oil and Gas Corrosion Research and Technologies*; Elsevier: Amsterdam, The Netherlands, 2017; pp. 3–30. [CrossRef]
8. McKenzie, M.; Vassie, P.R. Use of weight loss coupons and electrical resistance probes in atmospheric corrosion tests. *Br. Corros. J.* **1985**, *20*, 117–124. [CrossRef]
9. Wright, R.F.; Lu, P.; Devkota, J.; Lu, F.; Ziomek, M.M.; Ohodnicki, P.R., Jr. Corrosion Sensors for Structural Health Monitoring of Oil and Natural Gas Infrastructure: A Review. *Sensors* **2019**, *19*, 3964. [CrossRef] [PubMed]
10. Shin, D.H.; Hwang, H.K.; Kim, H.H.; Lee, J.H. Evaluation of commercial corrosion sensors for real-time monitoring of pipe wall thickness under various operational conditions. *Sensors* **2022**, *22*, 7562. [CrossRef]
11. Durrani, F.; Wesley, R.; Srikandarajah, V.; Eftekhari, M.; Munn, S. Predicting corrosion rate in chilled HVAC pipe network: Coupon vs linear polarisation resistance method. *Eng. Fail. Anal.* **2020**, *109*, 104261. [CrossRef]
12. Seghier, M.E.A.B.; Höche, D.; Zheludkevich, M. Prediction of the internal corrosion rate for oil and gas pipeline: Implementation of ensemble learning techniques. *J. Nat. Gas Sci. Eng.* **2022**, *99*, 104425. [CrossRef]
13. Seghier, M.E.A.B.; Keshtegar, B.; Tee, K.F.; Zayed, T.; Abbassi, R.; Trung, N.T. Prediction of maximum pitting corrosion depth in oil and gas pipelines. *Eng. Fail. Anal.* **2020**, *112*, 104505. [CrossRef]
14. Peng, S.; Zhang, Z.; Liu, E.; Liu, W.; Qiao, W. A new hybrid algorithm model for prediction of internal corrosion rate of multiphase pipeline. *J. Nat. Gas Sci. Eng.* **2021**, *85*, 103716. [CrossRef]
15. Dao, U.; Sajid, Z.; Khan, F.; Zhang, Y.; Tran, T. Modeling and analysis of internal corrosion-induced failure of oil and gas pipelines. *Reliab. Eng. Syst. Saf.* **2023**, *234*, 109170. [CrossRef]
16. Nassar, N.E.A. Corrosion in marine and offshore steel structures: Classification and overview. *Int. J. Adv. Eng. Sci. Appl.* **2022**, *3*, 7–11. [CrossRef]

17. Ji, H.; Wang, H.; Chen, Q.; Ma, X.; Cai, Y. Corrosion behavior prediction for hull steels under dynamic marine environments by jointly utilizing LSTM network and PSO-RF model. *Ocean Eng.* **2024**, *300*, 117371. [CrossRef]
18. Revie, R.W. *Corrosion and Corrosion Control: An Introduction to Corrosion Science and Engineering*; John Wiley & Sons: Hoboken, NJ, USA, 2008.
19. Biologic. VASP-RP Determination Corrosion Application Note. Available online: https://www.biologic.net/documents/vasp-rp-determination-corrosion-application-note-36/ (accessed on 12 October 2024).
20. Ilie, M.C.; Maior, I.; Raducanu, C.E.; Deleanu, I.M.; Dobre, T.; Parvulescu, O.C. Experimental Investigation and Modeling of Film Flow Corrosion. *Metals* **2023**, *13*, 1425. [CrossRef]
21. Tang, D.Z.; Du, Y.X.; Lu, M.X.; Liang, Y.; Jiang, Z.T.; Dong, L. Effect of pH value on corrosion of carbon steel under an applied alternating current. *Mater. Corros.* **2015**, *66*, 1467–1479. [CrossRef]
22. Yao, J.; Ge, H.; Zhang, Y.; Wang, X.; Xie, S.; Sheng, K.; Zhao, Y. Influence of pH on corrosion behavior of carbon steel in simulated cooling water containing scale and corrosion inhibitors. *Mater. Corros.* **2020**, *71*, 1266–1275. [CrossRef]
23. Chohan, I.M.; Ahmad, A.; Sallih, N.; Bheel, N.; Salilew, W.M.; Almaliki, A.H. Effect of seawater salinity, pH, and temperature on external corrosion behavior and microhardness of offshore oil and gas pipeline: RSM modelling and optimization. *Sci. Rep.* **2024**, *14*, 16543. [CrossRef]
24. Wang, Y.; Cheng, G.; Wu, W.; Qiao, Q.; Li, Y.; Li, X. Effect of pH and chloride on the micro-mechanism of pitting corrosion for high strength pipeline steel in aerated NaCl solutions. *Appl. Surf. Sci.* **2015**, *349*, 746–756. [CrossRef]
25. Huang, H.H.; Chuang, T.H. Erosion-and wear-corrosion behavior of Fe–Mn–Al alloys in NaCl solution. *Mater. Sci. Eng. A* **2000**, *292*, 90–95. [CrossRef]
26. Lee, S.J.; Han, M.S.; Jang, S.K.; Kim, S.J. Effect of flow velocity on corrosion rate and corrosion protection current of marine material. *Corros. Sci. Technol.* **2015**, *14*, 226–231. [CrossRef]
27. Zou, Y.; Wang, J.; Bai, Q.; Zhang, L.L.; Peng, X.; Kong, X.F. Potential distribution characteristics of mild steel in seawater. *Corros. Sci.* **2012**, *57*, 202–208. [CrossRef]
28. Jones, D.A. Principles and prevention. *Corrosion* **1996**, *2*, 168.
29. Darowicki, K. Corrosion rate measurements by non-linear electrochemical impedance spectroscopy. *Corros. Sci.* **1995**, *37*, 913–925. [CrossRef]
30. Diard, J.P.; Le Gorrec, B.; Montella, C. Corrosion rate measurements by non-linear electrochemical impedance spectroscopy. Comments on the paper by K. Darowicki, Corros. Sci. 37, 913 (1995). *Corros. Sci.* **1998**, *40*, 495–508. [CrossRef]
31. Cai, B.; Liu, Y.; Tian, X.; Wang, F.; Li, H.; Ji, R. An experimental study of crevice corrosion behaviour of 316L stainless steel in artificial seawater. *Corros. Sci.* **2010**, *52*, 3235–3242. [CrossRef]

Disclaimer/Publisher's Note: The statements, opinions and data contained in all publications are solely those of the individual author(s) and contributor(s) and not of MDPI and/or the editor(s). MDPI and/or the editor(s) disclaim responsibility for any injury to people or property resulting from any ideas, methods, instructions or products referred to in the content.